Pramana – J. Phys. (2019) 92:4
https://doi.org/10.1007/s12043-018-1664-4

Study of multiplicity dependence of pion fluctuations in π^-–AgBr collisions at 350 GeV using complex network approach

SUSMITA BHADURI*, ANIRBAN BHADURI and DIPAK GHOSH

Deepa Ghosh Research Foundation, 60/7/1 Maharaja Tagore Road, Kolkata 700031, India
*Corresponding author. E-mail: susmita.sbhaduri@dgfoundation.in

MS received 17 January 2018; revised 11 May 2018; accepted 18 May 2018; published online 26 October 2018

Abstract. A complex network and chaos-based method, based on the visibility graph algorithm, is applied to study particle fluctuations in π^-–AgBr interactions at 350 GeV with respect to the shower multiplicity dependence. The fractal structure of the fluctuations is studied by using the power of scale freeness of visibility graph (PSVG). The selection of visibility graph as the type of complex network for our analysis is justified as this algorithm gives the most precise result with finite number of data points and this experiment has finite number of events. The topological parameters along with PSVG values are extracted and analysed. The analysis shows that the fractality character is weaker for the lowest multiplicity bin and is stronger for the highest multiplicity bin.

Keywords. Complex network; visibility graph; high-energy collision; topological parameters; chaos-based nonlinear analysis.

PACS No. 25.80.Hp

1. Introduction

Multiparticle production has been the subject of immense interest for decades. Several theoretical, phenomenological and experimental attempts have been made to understand the dynamics behind this. Richer and richer data have come up, and also many models have been reported. However, as no conclusive understanding has been gained, many more sophisticated attempts are still being reported. One important aspect of the multiparticle production process is the correlation and fluctuation analysis with the help of which a great deal of rich information can be obtained. For the past several years, correlations and fluctuations have been studied but none of the studies revealed deterministic and thus important features. With the advent of different new approaches for studying non-statistical fluctuation, exhaustive work has been done yielding more in-depth understanding of this process.

The study of large density fluctuations in high-energy interactions has attained significant importance during the last decade, because of the ability of the large density fluctuations to supply interesting information on the dynamics of multiparticle production. Various methods were introduced for the analysis of large density fluctuations. Bialas and Peschanski [1] have attempted to examine multiplicity fluctuations in terms of scaled factorial moments which could not only detect large non-statistical fluctuations but also analyse the pattern of fluctuations, eventually leading to the physical interpretation of their origin. It was suggested that the nature of factorial moments is analogous to the phenomenon called intermittency in hydrodynamics of turbulent fluid flow. Intermittency is a mechanism that creates strong local fluctuations in uniform and large statistical systems. The underlying physical reason of intermittency has been the self-similarity of the system in question over a range of scales. It has been observed that the multipion production process in heavy-ion interaction shows a power-law behaviour of the factorial moments with respect to the size of phase-space intervals in a decreasing mode. An indication of a self-similar fluctuation is thereby obtained, which in turn indicated the fractal behaviour in multipion production process. Bialas and Peschanski [1] also indicated a relationship between the fractality and intermittency. The study of fractal behaviour of multipion production from the perspective of intermittent fluctuations using the method of factorial moment had been an initial area of interest. In this context, it is worth mentioning about a simple relationship between the anomalous fractal

dimension and intermittency indices [2,3]. The cascading mechanism inherent in the multipion production process produces a fractal structure as a natural consequence. The scale invariance present in the hadronisation process has also been evident from the spectrum of fractal dimensions.

In the recent past, numerous techniques based on the fractal theory have been implemented to analyse the process of multipion emission [4–8]. The most popular of them have been Gq moment and Tq moment developed by Hwa [4] and Takagi [8]. The Gq moments were calculated to extract fractal properties of the multiplicity distributions by Hwa. However, the Gq moments are affected by statistical fluctuations in the case of lower event multiplicity. Takagi proposed another concept of Tq moments that are not specifically affected by lower event multiplicity. Takagi pointed out that conventional methods do not extract the expected linear behaviour in a log–log plot as those methods cannot satisfy the required mathematical limit where the number of points tends to infinity.

Various natural systems can be interpreted as complex heterogeneous systems which consist of different kinds of elementary units that can communicate among themselves through diverse interactions (both long-range and short-range). Hence, apart from fractal and multifractal approaches, recently new approaches have been proposed to represent complex systems in terms of complex networks as complex network-based methods provide us a quantitative model for large-scale natural systems (in fields of biology, physics and social sciences). The topological properties of the complex networks derived from the real systems provide useful information about the characteristics of the system. Network science has hugely evolved in the past two decades, and is nowadays a prominent scientific field in the area of complex systems, which includes every feature of our daily life [9–11].

Lacasa *et al* [12,13] have introduced visibility graph analysis method, which has gained importance due to its entirely different, rigorous approach to assess fractality. Recently, using visibility graph method, multiplicity fluctuation has been analysed in π^-–AgBr (350 GeV) and ^{32}S–AgBr (200 A GeV) interactions [14,15] and also the fractality of void probability distribution has been analysed in ^{32}S–AgBr interaction at an incident energy of 200 GeV per nucleon [16–18].

As the dynamics of multiparticle production with respect to its multiplicity dependence is yet to come out with deterministic parameters and details, various topological parameters derived from the complex network analysis of this process should give more and more insight about the dynamics and that too from substantially different perspective. Inspired by the interesting findings observed in the above studies using the complex network approach (visibility graph method), in this work the π^-–AgBr (350 GeV) interaction data have been further analysed in-depth, precisely the shower-multiplicity dependence [represented by increasing range of shower multiplicity dependence (denoted by n_s) of the interaction data] of the pionisation process, using the visibility graph algorithm and then extracting all the topological parameters from the graphs. We have studied the fractal behaviour of the process by utilising the method's scale-freeness detection mechanism, that is by extracting and analysing the power of scale freeness of visibility graph (PSVG) denoted by λ_p which indicates the amount of self-similarity and in effect the fractal dimension of the experimental data series [12,13,19]. Also, it has been observed that there is an inverse linear relationship between the PSVG and Hurst exponent of the experimental data series [13]. Apart from PSVG, the topological parameters, such as heterogeneity index [20] (here denoted by H), average clustering coefficient [21] (here denoted by C), average degree [22] (here denoted by D), average shortest path [23] (here denoted by P) and assortativity coefficient [24] (here denoted by A), are extracted from the visibility graphs formed out of the datasets of the interaction for each range of n_s. Then, we have analysed the results with respect to the parameters' physical significance relevant for multiparticle production process and its shower multiplicity dependence. We emphasise here again that as a finite number of events are available in this experiment, use of the visibility graph technique is well justified. Apart from the regular significance of these parameters, normally derived from and implemented in complex network, one can correlate their physical significance with some fundamental concepts in particle production phenomenology, such as correlation, clustering, correlation length, etc. With the help of these new parameters, one can analyse the multipion data more rigorously and robustly and eventually quantify non-statistical fluctuations, which have a strong bearing on the multiparticle production process.

The rest of the paper is organised as follows. The method of visibility graph algorithm and the significance of complex-network parameters including scale-freeness property are presented in §2. The detailed data description and related terminologies are elaborated in §3.1. The details of our analysis and the inferences from the test results are given in §3.2. The physical significance of the network parameters and their prospective correlation with the traditional concepts of multiparticle production process with respect to its multiplicity dependence is elaborated and the paper is concluded in §4.

2. Method of analysis

The visibility graph algorithm converts a time or data series into a graph, which naturally inherits various properties of the series in its structure. Periodic series gets transformed into regular graphs and random series into random graphs. Fractal series gets transformed into scale-free networks (with power-law degree distributions), intensifying the fact that power-law degree distributions are related to fractality. A scale-free visibility graph is formed from data points of a fractal time series, based on the visibility between the nodes of the time or data series [13].

The visibility graph method is briefly described in this section.

2.1 *Visibility graph algorithm*

The visibility graph algorithm [12,13,19] plots time series X to its visibility graph. Let us assume that the ith point of time series is X_i. In the constructed graph, two nodes or vertices (X_m and X_n corresponding to mth and nth points in the time series) are supposed to be visible to each other or in other words, connected by a two-way edge if and only if eq. (1) is satisfied:

$$X_{m+j} < X_n + \left(\frac{n-(m+j)}{n-m}\right)\cdot(X_m - X_n), \qquad (1)$$

where $\forall j \in Z^+$ and $j < (n-m)$.

It is shown in figure 1 that the nodes X_m and X_n, where $m = i$ and $n = i+6$, can be visible to each other only if eq. (1) is valid. It is evident that two sequential points of the time series can always see each other and thereby sequential nodes are always connected.

2.1.1 *Network parameters.* The network parameters to be extracted from the visibility graphs constructed from each of the experimental data series are elaborated below.

1. *Heterogeneity index*: The networks with Poissonian degree distribution are considered as almost regular networks where most of the nodes have nearly the same degree, and a few of them have very high or small degrees. But these variations are very high for a scale-free network. For a scale-free network, the probability of finding very small degree nodes is very high, whereas very few nodes have very large degrees. In scale-free and star networks, there exist remarkably higher degree nodes than the average degree of the network. This structural feature reflects their irregularity which is known as their *heterogeneity* [25]. To determine the network heterogeneity quantitatively, this parameter is extracted from a network which in this case is the visibility network. The normalised heterogeneity index is calculated as per eq. (2), defined by Estrada [20] and Ye *et al* [26],

$$\rho(G) = \frac{\sum_{i,j\in E}(k_i^{-1/2} - k_j^{-1/2})^2}{n - 2\sqrt{n-1}}, \qquad (2)$$

where $\sum_{i,j\in E}(k_i^{-1/2} - k_j^{-1/2})^2$ is the the sum of the link irregularity for all links in the network and link irregularity is defined for each link or edge $(i, j) \in E$, connecting ith and jth nodes as $[f(k_i) - f(k_j)]^2$, where $f(k_i)$ is a function of a node degree. Here, $f(k_i)$ has been taken as $k_i^{-1/2}$ where k_i is the degree of the ith node.

To determine the network heterogeneity quantitatively, this parameter is extracted from a network which in this case is the visibility network. The normalised heterogeneity index is calculated as per eq. (2), defined by Estrada [20] and Ye *et al* [26]. The value of this parameter falling in the range between moderate and high value, as specified in [20], characterises the network as moderately heterogeneous or a highly heterogeneous. It can also be validated whether the range of values of the indexes confirms to the scale-free property of the visibility network or not.

2. *Average clustering coefficient*: Clustering coefficient is the estimation of the extent to which nodes of a graph incline to cluster together. The average clustering coefficient has been defined by Watts and Strogatz [21] as the overall clustering coefficient of a network, which is estimated as the mean local clustering coefficient of all the nodes in the network.

A graph $G = (V, E)$ consists of a set of vertices V and another set of edges E between them. An edge $e_{ij} \in E$ connects vertices v_i and v_j. The neighbourhood N_i for any vertex $v_i \in V$ is defined as its neighbours which are immediately connected to it, denoted by $N_i = \{v_j : e_{ij} \in E \vee e_{ji} \in E\}$. Watts and Strogatz have defined the local

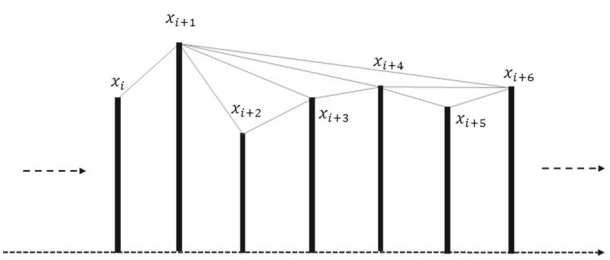

Figure 1. Visibility graph for the time series X.

clustering coefficient, denoted by C_i for the vertex v_i, as the number of links existing between the vertices within its neighbourhood divided by the number of links that can probably exist between them. For the directed graph, e_{ij} is different from e_{ji}. So, for each neighbourhood N_i corresponding to each vertex v_i there can exist a maximum of $k_i(k_i-1)$ number of links among the vertices within N_i, where k_i is the number of elements in the set N_i, or the number of neighbours of v_i. In this case, C_i is defined by

$$\frac{\left|\{e_{jk} : v_j, v_k \in N_i, e_{jk} \in E\}\right|}{k_i(k_i-1)}.$$

For the undirected graph e_{ij} is identical to e_{ji}, and so v_i has k_i number of neighbours in N_i and maximum of $(k_i(k_i-1))/2$ number of edges may exist among the vertices within N_i. Hence, C_i is defined by

$$\frac{2\left|\{e_{jk} : v_j, v_k \in N_i, e_{jk} \in E\}\right|}{k_i(k_i-1)}.$$

Then the average clustering coefficient of a network, denoted by $\bar{C}$, is calculated by averaging the local clustering coefficients for all the vertices in the networks.

In this experiment, the criteria for clustering are the tendency of the nodes in the visibility graphs to be visible to each other. Hence, the existence of a path or edge between neighbours of a particular node in the graph is decided by its visibility to each other. The more visible the neighbour nodes are to each other, the more correlated and clustered they are, for a particular node. This way, for each node, the correlation between its neighbour nodes is calculated and finally the average clustering coefficient of the particular visibility graph is measured. High value of this coefficient indicates the robustness of a network.

3. *Average degree*: The degree of a vertex (node) of a graph is the number of edges connected to it within the graph. The degree of each vertex is defined as the number of edges that enter or exit from it [22]. So, a loop in a vertex brings about 2 to its degree. The sum of degrees of the vertices of a graph (denoted by $G = (V, E)$ with a set of vertices V and another set of edges E between them) is defined by $\sum_{v\in V} \deg(v) = 2|E|$.

   The average degree is defined by $(\sum_{v\in V} \deg(v)/|V|)$, where $|V|$ is the total number of vertices of the graph. In this experiment, an edge between a pair of nodes in the visibility graph is defined as per the visibility of the nodes to each other. This parameter globally quantifies the property of a graph, which is estimated locally by the node degrees of the graph [22].
4. *Average shortest path*: The average number of steps among the shortest paths for all probable pairs of nodes of the network is termed as the average shortest path. It is calculated as per the method proposed by Johnson [23] and it measures the effectiveness of transport of information through the network.

   As per Johnson's algorithm, to calculate the average shortest path of a graph, first a vertex v_q is added to the graph, which is connected by zero-weight edges to each of the existing vertices in the graph. Then the Bellman–Ford algorithm is used, starting from v_q, to find minimum weight $h(v_i)$ of a path (if exists) from v_q to v_i for each vertex v_i in the graph. Then the edges of the original graph are reweighted using the values computed by the algorithm. For example, an edge from v_a to v_b, having length $w(v_a, v_b)$ is updated to a new length $w(v_a, v_b)+h(v_a)-h(v_b)$. Ultimately, v_q is removed and Dijkstra's algorithm is applied to find the shortest paths from each vertex to every other one in the reweighted graph.
5. *Assortativity coefficient*: If the edges of the graph normally appear between its nodes of the same type, the graph is assortative, whereas the graph is said to be disassortative if its edges generally appear between different types of nodes. So, we can deduce that the assortativity coefficient of the graph (here the visibility graph) is the estimation of correlation of degree between pairs of linked nodes. Here, the degree of the nodes is considered as the type of correlation to be measured.

   We have calculated the assortativity coefficient s for the visibility graphs according to eq. (3) proposed by Newman [24]. Newman has defined assortativity by the Pearson correlation coefficient, here denoted by r:

$$r = \frac{M^{-1}\sum_i j_i k_i - [M^{-1}\sum_i \frac{1}{2}(j_i+k_i)]^2}{M^{-1}\sum_i \frac{1}{2}(j_i^2+k_i^2) - [M^{-1}\sum_i \frac{1}{2}(j_i+k_i)]^2}. \tag{3}$$

   Here M is the number of edges in the graph, j_i, k_i are the degrees of the vertices of the ith edge, with $i = 1, 2, \ldots, M$.

2.1.2 *Power of scale-freeness of VG – PSVG.* The degree of a node or vertex in a graph, here the visibility graph, is the number of connections or edges the node has with the rest of the nodes in the graph. The degree distribution $P(k)$ of a network is therefore defined as

the fraction of nodes with degree k, with respect to the total number of nodes present in the network. So, if there are n_k number of nodes in the network, having degree k and total number of nodes in total in a network is n, then we define $P(k) = n_k/n$ for all possible values of k. In our experiment for each visibility graph constructed from the data series corresponding to each of the experimental datasets, k vs. $P(k)$ dataset is generated for all possible values of k.

As per Lacasa *et al* [12,13] and Ahmadlou *et al* [19], the degree of scale-freeness of a visibility graph corresponds to the amount of fractality and complexity of the data series. According to the scale-freeness property of the visibility graph, the degree distribution of its nodes should follow the power law, i.e. $P(k) \sim k^{-\lambda_p}$.

3. Experimental details

3.1 *Data description*

The data used in our experiment are obtained from one of the analysis of CERN, where Illford G5 emulsion plates are exposed to a π^--beam of 350 GeV incident energy from CERN. A Leitz Metaloplan microscope with 10× ocular lens, equipped with an additional semi-automatic scanning stage, was used to analyse the plate. Each plate was analysed by two independent observers to maximise the accuracy in detection, counting and measurement process. Hence, the scanning efficiency could be increased. For the final measurement, an oil immersion-10× objective was used. The measuring system was unified with two microscopic systems having the specification of 1 μm resolution along the X- and Y-axes, and 0.5 μm resolution along the Z-axis.

In our previous works [14,15,27], the criteria for event section are already explained. In the context of nuclear emulsion [28], after the interactions, the discharged particles are catalogued as shower, grey and black particles, which are defined as follows.

1. *Shower particles*: The minimum ionisation of a singly charged particle is denoted by I_0. If the ionisation of the particle is less than or equal to $1.4I_0$, then those particles are called shower particles which are mostly generated by combining pions with a small admixture of K-mesons and fast protons. The velocity of these particles is more than $0.7c$, with c representing the speed of light in free space.
2. *Grey particle*: Grey particles generally consist of some knocked-out protons with energy level of 30–400 MeV, slow pions with energy level of 30–60 MeV and admixture of deuterons and tritions. Their ionisation level is between $1.4I_0$ and $10I_0$. These particles have velocity between $0.3c$ and $0.7c$ and have ranges more than 3 mm in the emulsion medium.
3. *Black particles*: These particles are also termed as target fragments, which consist of both singly and multiply charged fragments. Their ionisation is greater than or equal to $10I_0$ and they consist of fragments of various elements such as carbon, lithium, beryllium, etc. These particles have short ranges, less than 3 mm in the emulsion medium. Their ionisation power is maximum and they are less energetic and are very short ranged. Their velocities are less than $0.3c$.

3.2 *Method of analysis*

In this analysis, the total number of events of experimental interaction has been divided into four windows of n_s-ranges, as per the increasing average shower multiplicity or average of event-wise shower count for each of the ranges. The event-wise shower count or shower multiplicity denoted by n_s has been noted and the number of events is grouped in such a way that in each group the average shower count (n_s) of the events is in ascending order. For example, in the first group events with lowest range of n_s is selected. This group contains around 80 events and the count of pseudorapidity (η) values for each of those events ranges from 0 to 10. Hence, the average multiplicity or the average of event-wise n_s values in that group is 7. In a similar manner, the rest of the n_s ranges is decided.

Although, in doing so, the number of events in some cases of experimental data has become comparatively low, the visibility graph method can extract PSVG and other network parameters, reliably with short data, even with 400 data points [29] and therefore this does not affect the result of the analysis.

Using four datasets for the interaction, we have then done a comparative analysis between all the parameters extracted from the visibility graph analysis, as explained in §2.1.1 and 2.1.2. Furthermore, we have also studied how these parameters vary from one n_s range to another. Detailed steps of our analysis are elaborated below.

The pseudorapidity (η) values available for each of the events are extracted. Thus, we get four data series of η-values for four groups of events corresponding to each of the four shower multiplicity (n_s) ranges. Table 1 shows n_s ranges for experimental data and average shower multiplicity in each group. n_s ranges are decided in such a manner that the average number of events in each range is similar. Figure 2 shows the trend of η-values for each of the four n_s ranges.

Then, for each data series of η values extracted for each range of n_s, visibility graphs are constructed for each of these datasets and for each of the visibility graphs the topological parameter, as listed in §2.1.1, and PSVGs are extracted.

3.2.1 *Monte–Carlo simulation for the complex-network parameters.* We have repeated the visibility graph analysis as per the method described in §2 and then extracted the topological parameters and PSVG from the graphs constructed from the randomised (shuffled) version of the experimental data. Then, we have produced Monte–Carlo events assuming independent emission of pions in the experimental data. Monte–Carlo events have been chosen in such a manner that $dn/d\eta$ distribution of Monte–Carlo-simulated events follows the corresponding $dn/d\eta$ of the real ensembles. We have repeated the same method of analysis as described in §2 with these Monte–Carlo-generated events and extracted the same parameters.

Then we have compared the network parameters and PSVG values calculated for the

1. experimental data (Exp),
2. Monte–Carlo-generated events (MC),
3. randomised data (RN).

Table 1. n_s ranges for experimental data and average multiplicity in each group.

Average shower multiplicity	n_s ranges
7 ± 2	$0 < n_s \leq 10$
12 ± 1	$10 < n_s \leq 13$
15 ± 1	$13 < n_s \leq 17$
21 ± 3	$17 < n_s \leq 28$

The analysis of all the parameters is given in §3.2.2 and 3.2.3. The statistical errors calculated for all the network parameters by following the standard process are shown in tables 1–4, the details of which are already elaborated in earlier works e.g. [30]. Pearson's chi-squared test [31] method is followed to calculate $\chi^2_{\text{exp}}/\text{DOF}$ values after considering the statistical errors. It is also necessary to analyse the effect of systematic errors in the analysis. Like other detectors, nuclear emulsion plates are also not devoid of systematic errors. Cosmic rays emitted during the exposure of the emulsion plates result in background events which may infuse systematic errors. In our experiment, these background events were removed by choosing the primary events precisely. The variation of shrinkage factor and the fading of tracks with temperature variations may also infuse systematic errors in the measurement of polar angles. However, as these errors are relatively smaller, they do not influence the final results. Further, it is well established that the emulsion detector gives the highest spatial resolution and by following the standard procedures (e.g. using multiple scanners) the scanning efficiency can also be optimised.

3.2.2 *Analysis of network parameters of the visibility graphs.*

1. *Heterogeneity index (H)*: This parameter is calculated for all the visibility graphs as per the method prescribed by Estrada [20] and Ye *et al* [26]. The heterogeneity indexes are extracted for all the visibility graphs, as per the method described in §2.1.1 and listed in table 2. Table 2 shows that for all ranges of n_s, the constructed visibility graphs are moderately heterogeneous. Further, the range of values of the indexes confirms to the scale-free property of the visibility

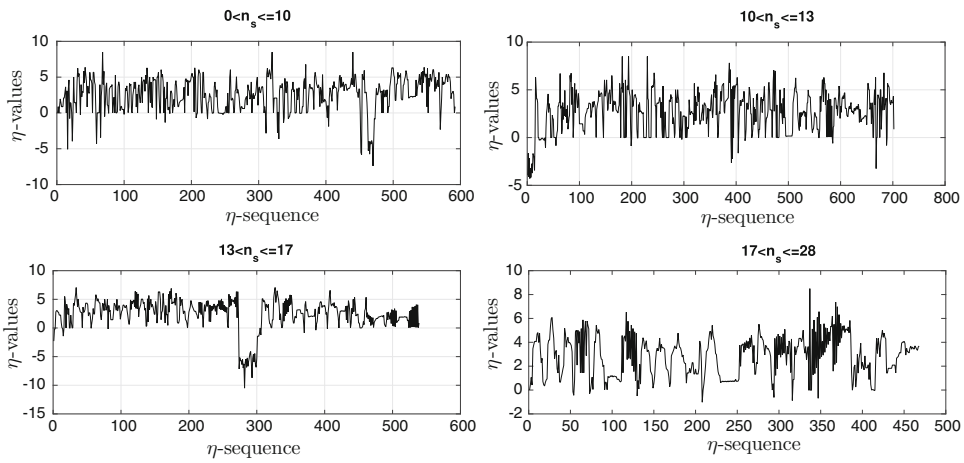

Figure 2. Data series of the four n_s ranges of the experimental data.

graphs [20] and also the visibility graphs constructed for the third and fourth n_s ranges are the most heterogeneous. Table 2 shows that the values of the index of experimental result are moderately greater than those of Monte–Carlo-simulated and randomised events.

2. *Average clustering coefficient (C)*: As already discussed in §2.1.1, this parameter indicates the probability of the neighbour nodes of a node in a graph to be also neighbours to each other or not. Average clustering coefficients for the four visibility graphs are calculated as per the method prescribed by Watts and Strogatz [21] and listed in table 2. It is evident from table 2 that the average clustering coefficient of the visibility graph is maximum for second and fourth ranges of n_s and same for the rest of the two ranges, whereas the value of this parameter is almost consistent across all the n_s ranges for the randomised and Monte–Carlo-simulated versions of the data. Table 2 shows that the experimental result is substantially more than that of the Monte–Carlo-simulated events and also randomised version of the events.
3. *Average degree (D)*: As discussed in §2.1.1, this parameter quantifies the density of a graph with respect to its nodes and their edges. Comparison of the average degree of the four visibility graphs formed from each dataset is shown in table 2. It is evident that average degree is minimum for the first n_s range, maximum for the fourth n_s range and almost similar for the rest of the ranges. Table 2 shows that the experimental result is substantially more than that of both Monte–Carlo-simulated events and the randomised version of the events.
4. *Average shortest path (P)*: From the discussion in §2.1.1, we understand that this parameter signifies how efficiently one can reach from one node to another in the graph. In other words, it measures whether the nodes are correlated or connected in the more direct manner or via several other nodes. The average shortest paths between the nodes of

Table 2. Trend of heterogeneity index, Avg. clustering coeff. and Avg. degree for the visibility graphs extracted from the actual data, their randomised and Monte–Carlo-simulated versions for each of the four datasets of η-values for four ranges of n_s as per table 1 for experimental data.

n_s	*H*			*C*			*D*		
	Exp.	MC	RN	Exp.	MC	RN	Exp.	MC	RN
7	0.21 ± 0.04	0.19	0.20	0.41 ± 0.01	0.32	0.32	9.72 ± 0.23	7.41	7.21
12	0.23 ± 0.03	0.21	0.21	0.46 ± 0.01	0.34	0.33	11.65 ± 0.24	7.58	7.32
15	0.25 ± 0.04	0.20	0.21	0.41 ± 0.01	0.33	0.33	10.96 ± 0.26	7.51	7.47
21	0.25 ± 0.05	0.20	0.21	0.45 ± 0.01	0.32	0.31	12.75 ± 0.35	7.59	7.13

Table 3. Trend of average shortest path length and assortativity coefficient for the visibility graphs extracted from the actual data, their randomised and Monte–Carlo-simulated versions for each of the four datasets of η-values for four ranges of n_s as per table 1 for the experimental data.

n_s	*P*			*A*		
	Exp.	MC	RN	Exp.	MC	RN
7	4.813 ± 0.003	7.75	5.00	0.31 ± 0.04	0.26	0.19
12	5.055 ± 0.003	8.09	5.30	0.33 ± 0.04	0.23	0.16
15	4.630 ± 0.003	8.11	5.00	0.27 ± 0.04	0.21	0.13
21	4.311 ± 0.003	7.15	4.60	0.32 ± 0.05	0.27	0.17

Table 4. Trend of PSVG-λ_p for the visibility graph extracted from the actual datasets of η-values for four ranges of n_s as per table 1 for the experimental data, their randomised versions and their Monte–Carlo-simulated versions.

n_s	PSVG experimental-λ_p	χ^2/DOF	R^2	PSVG-MC-simulated-λ_{mc}	PSVG randomised-λ_{rn}
7	2.66 ± 0.1	0.04	0.93	3.69	2.81
12	2.30 ± 0.1	0.01	0.95	3.33	2.77
15	2.33 ± 0.2	0.02	0.91	3.36	2.68
21	2.22 ± 0.2	0.03	0.84	3.46	2.70

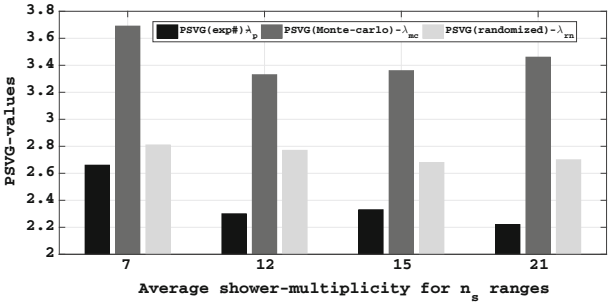

Figure 3. Comparison of PSVG values calculated for the visibility graphs created for four datasets for each range of n_s as per table 1 for experimental, randomised and Monte–Carlo-simulated versions of the events.

the four visibility graphs are calculated as per the method proposed by Johnson [23] and listed in table 3. It is highest for the visibility graph created for the second range of n_s and lowest for the fourth range and the experimental result is substantially less than Monte–Carlo-simulated events and moderately less than the randomised version of events.

5. *Assortativity coefficient (A)*: We deduce from §2.1.1 that the assortativity coefficient of the visibility graph is the measure of correlation of degree parameter between pairs of linked nodes. Assortativity coefficients for the four visibility graphs are calculated as per the method suggested by Newman [24] and listed in table 3. It is evident that all the four graphs are highly assortative except the third one which is moderately assortative. Table 3 shows that the experimental result is moderately more than that of the Monte–Carlo-simulated events and substantially more than that of the randomised version of the events.

3.2.3 *Analysis of power of scale-freeness of the visibility graphs.* For each of the four visibility graphs constructed for the four ranges of n_s as per table 1 for the experimental data, the k vs. $P(k)$ datasets are calculated as per the method described in §2.1.2. The power-law index has been obtained by power-law fitting for the k vs. $P(k)$ datasets as per the method prescribed by Clauset *et al* [32]. The power-law relationship can be confirmed from the corresponding χ^2_{exp}/DOF values and the values of R^2. We can also confirm scale-freeness property of the visibility graph constructed for each dataset, from the range of heterogeneity index (H) values in table 2. This in turn confirms the scale-freeness property inherent in each dataset from which the visibility graphs are constructed. As already mentioned in §2.1.2, the degree of scale-freeness of the visibility graph corresponds to the amount of fractality and complexity of the experimental data series.

The PSVG denoted by λ_p is calculated from the slope of $\log_2[1/k]$ vs. $\log_2[P(k)]$ for all the visibility graphs constructed. The same value for λ_p has been obtained by power-law fitting done for the corresponding k vs. $P(k)$ dataset. The PSVG measures complexity and fractality of the data series and in turn indicates the fractal dimension of the data series [12,13,19].

Table 4 lists λ_p values along with the corresponding χ^2/DOF and R^2 values for the datasets for four ranges of n_s for the experimental data. λ_p is maximum for the first range, minimum for the fourth range and remains more or less the same for the rest of the ranges. Both table 4 and figure 3 show that the values of PSVGs calculated for the experimental result are significantly less than that of the Monte–Carlo-simulated and randomised versions of events. From the analysis of the PSVG, one can quantitatively confirm that the fractal behaviour of the particle production process depends on the shower multiplicity and the fractality decreases with the increase of shower multiplicity, observation of which is interesting and useful for further modelling of the dynamics of multiparticle production in high-energy collisions. Further, this dependence of pion fluctuation on multiplicity has been reported by other parameters in many works (e.g. see [33] and reference therein).

We may mention that all the above parameters hint similar nature of dependence of pion fluctuation on multiplicity except for a few cases where this nature is not reflected with the inclusion of error. However, the overall analysis is not perturbed by this.

4. Conclusions

- In this work, a chaos-based, rigorous, nonlinear and complex network-based technique named visibility graph algorithm is presented and the topological parameters including the PSVG of the constructed graphs are extracted to study the fluctuation of pions in high-energy collisions. In this analysis π^-–AgBr interactions at 350 GeV are studied.
- The comparison of the parameters among experimental, randomised and Monte–Carlo-simulated ensembles establishes that the PSVG and the topological parameters – *H, C, D, P* and *A* calculated for the randomised or Monte–Carlo-simulated fluctuation patterns – do not reproduce the experimental result exactly. They are indicative of inherent features involved in pionisation process with respect to shower-multiplicity dependence. The range of H's and power-law trend of the degree distribution pattern manifested out of pionisation process, for each of the n_s range, confirm to the scale-freeness property [34] of the process. The tables also indicate the

degree of scaling behaviour or λ_p is maximum at the first n_s ranges and minimum in the last one.

- The higher range of C and lower range of P for all four ranges confirm to the small-world properties of the complex networks [21]. Higher ranges of A for n_s ranges (barring the third one) signify that there exists strong correlation between the nodes of similar degree [24].
- One may interpret complex network parameters as manifestors of conventional characteristics of multiparticle production process (such as clans, etc.) and thus utilise C to differentiate the types of clusters formed for different visibility graphs for different ranges of n_s and D can be correlated with the number of particles (nodes) in a cluster. P may be associated with the correlation length from node to node.
- It is interesting to note that the trend of C, A, P and D is remarkably similar from lower to higher n_s range, as all these parameters are dependent on the correlation between the nodes with respect to their degrees inside the clusters formed in the visibility networks.

This study of scaling behaviour from a new perspective is a first of its kind analysis in the domain of high-energy pionisation process yielding interesting, reliable results giving clues for finding new features of the process of pion production in high-energy interaction. In the case of some parameters, the small difference between the randomised or Monte–Carlo-simulated values and the experimental ones is the outcome of data sample size, for which it is difficult to draw any conclusion on the dynamics. However, the method may be used for large datasets where one can reach a confident conclusion about the dynamics. It is further expected that the values of the PSVG and network parameters would also be significantly different in the soft process, compared to the hard process. These parameters may also be indicative of phase transition if remarkable change is identified in any or all these parameters. This analysis can be extended with data of other high-energy interactions of different projectiles and energies.

Acknowledgement

The authors thank the Department of Higher Education, Government of West Bengal, India, for logistics support of computational analysis.

References

[1] A Bialas and R Peschanski, *Nucl. Phys. B* **273**, 703 (1986)
[2] A Bialas and R Peschanski, *Nucl. Phys. B* **308**, 857 (1988)
[3] E De Wolf, I Dremin and W Kittel, *Phys. Rep.* **270**, 1 (1996)
[4] R Hwa, *Phys. Rev. D* **41**, 1456 (1990)
[5] A V G Paladin, *Fractals* **3(4)**, 785 (1995)
[6] I P P Grassberger, *Physica D* **13**, 34 (1984)
[7] M J T C Halsey, L Kadanoff, I Procaccia and B Shriman, *Phys. Rev. A* **33**, 1141 (1986)
[8] F Takagi, *Phys. Rev. Lett.* **72**, 32 (1994)
[9] M Newman, A Barabasi and D Watts (Eds), *The structure and dynamics of networks* (Princeton University Press, 2006)
[10] S Boccaletti, V Latora, Y Moreno, M Chavez and D Hwang, *Phys. Rep.* **424**, 175 (2006)
[11] R Cohen, *Complex networks structure, robustness and function*, 1st edn (Cambridge University Press, 2014)
[12] L Lacasa, B Luque, F Ballesteros, J Luque and J C Nuno, *Proc. Natl Acad. Sci.* **105**, 4972 (2008)
[13] L Lacasa, B Luque, J Luque and J C Nuno, *Europhys. Lett.* **86(3)**, 30001 (2009)
[14] S Bhaduri and D Ghosh, *Int. J. Mod. Phys. A* **31**, 1650185 (2016)
[15] S Bhaduri and D Ghosh, *Acta Phys. Pol. B* **48**, 741 (2017)
[16] S Bhaduri and D Ghosh, *Mod. Phys. Lett. A* **31**, 1650158 (2016)
[17] S Bhaduri, A Bhaduri and D Ghosh, *Eur. Phys. J. A* **53**, 135 (2017)
[18] A Bhaduri, S Bhaduri and D Ghosh, *Phys. Part. Nucl. Lett.* **14**, 576 (2017)
[19] M Ahmadlou, H Adeli and A Adeli, *Phys. A: Stat. Mech. Appl.* **391(20)**, 4720 (2012)
[20] E Estrada, *Phys. Rev. E* **82**, 066102 (2010)
[21] D J J Watts and S H H Strogatz, *Nature* **393**, 440 (1998)
[22] S C Carlson, *Graph theory*, https://doi.org/10.1007/978-1-84628-970-5 (2014)
[23] D B Johnson, *J. ACM* **24**, 1 (1977)
[24] M E J Newman, *Phys. Rev. Lett.* **89**, 208701 (2002)
[25] R Albert and A-L Barabási, *Rev. Mod. Phys.* **74**, 47 (2002)
[26] C Ye, R C Wilson, C H Comin, L da F Costa and E R Hancock, *Entropy and heterogeneity measures for directed graphs* (Springer, Berlin, Heidelberg, 2013)
[27] A D Dipak Ghosh, S Bhattacharyya and U Datta, *J. Phys. G* **39(3)**, 035101 (2012)
[28] C F Powell, P H Fowler and D H Perkins, *The study elementary particles by the photographic method* (Pergamon Press, Oxford, 1959)
[29] S Jiang, C Bian, X Ning and Q D Y Ma, *Appl. Phys. Lett.* **102(25)**, 253 (2013)
[30] D Ghosh, A Deb, S Bhattacharyya and U Datta, *Phys. Scr.* **85(6)**, 065205 (2012)
[31] K Pearson, *Philos. Mag. Ser. 5* **50(302)**, 157 (1900)
[32] A Clauset, C R Shalizi and M E J Newman, *SIAM Rev.* **51**, 661 (2009)
[33] D Ghosh, A Deb and S Dutta, *Can. J. Phys.* **86(5)**, 751 (2008)
[34] A-L Barabási, *Nature Phys.* **8**, 14 (2011)